

# Probing the electronic structure of mono-nitrogen doped aluminum clusters using anion photoelectron spectroscopy

X. Li and L.-S. Wang<sup>a</sup>

Department of Physics, Washington State University, 2710 University Drive, Richland, Washington 99352, USA  
and

Chemical Sciences Division, Pacific Northwest National Laboratory, MS K8-88, Richland, Washington 99352, USA

Received 6 September 2004

Published online 13 July 2005 – © EDP Sciences, Società Italiana di Fisica, Springer-Verlag 2005

**Abstract.** We report a photoelectron spectroscopic investigation of mono-nitrogen doped aluminum cluster anions  $\text{Al}_n\text{N}^-$  ( $n = 2-22$ ). Well-resolved spectra were obtained at three photon energies (355, 266, and 193 nm), revealing the structural and electronic evolution as the number of aluminum atoms increases in the doped clusters. For small  $\text{Al}_n\text{N}$  ( $n < 9$ ) clusters, the Al atoms may be viewed to be monovalent, similar to pure aluminum clusters. Even-odd alternation of the electron affinities was observed for  $\text{Al}_n\text{N}$  clusters, suggesting that neutral clusters with odd  $n$  are closed shell and those with even  $n$  are open shell. The most interesting observation is the similarity between the spectra of  $\text{Al}_n\text{N}^-$  and  $\text{Al}_{(n-1)}^-$  for  $n > 12$ .

This observation suggests that these clusters can be described as  $(\text{AlN})\text{Al}_{(n-1)}^-$ , i.e., an AlN unit weakly interacting with  $\text{Al}_{(n-1)}^-$  clusters. The electronic and atomic structural implications of this observation are discussed.

**PACS.** 36.40.Mr Spectroscopy and geometrical structure of clusters – 33.60.Cv Ultraviolet and vacuum ultraviolet photoelectron spectra

## 1 Introduction

The electronic structure of aluminum in its bulk form is very different from that in clusters [1,2]. In bulk, trivalent aluminum is a nearly free electron metal [3]. Small aluminum clusters containing less than nine atoms has been found to behave as a monovalent atom [4], due to its large energy gap of 3.6 eV between the  $3s$  and  $3p$  states [5]. As is well known, the electronic structure of alkali metal clusters can be described by the electron-shell model [6–8]. In this model, valence electrons of the metal atoms are delocalized in the volume of the clusters and move in a spherical Jellium potential created by the ionic cores. The electrons are quantized according to the spherical orbitals, leading to the well-known electron shell structures. Shell structures were first observed in the mass spectra of  $\text{Na}_n$  clusters [6], where particularly abundant clusters (magic numbers) were observed at  $n = 8, 20, 40, 58, \text{ and } 92$ . Like alkali metal clusters the electronic structure of Al clusters containing up to 75 atoms were observed to be described by the Jellium model [4].

The electrons in nitrogen, on the other hand, form ionic and covalent bonds. Aluminum nitride (AlN) in its bulk form is a semiconductor with a large band-gap

(6.2 eV) and is an excellent thermal conductor [9,10]. The bonding characteristic in bulk aluminum nitride is partially ionic and partially covalent with each nitrogen atom surrounded by aluminum atoms. However, much less information is available on how the bonding of nitrogen with metal atoms such as aluminum atoms evolves from clusters to crystals. What is little known is how the electronic and geometrical structures evolve in mono-nitrogen doped aluminum clusters ( $\text{Al}_n\text{N}$ ). Some typical considerations are as follows. Does aluminum still behave as a monovalent atom while reacting with nitrogen in small  $\text{Al}_n\text{N}$  ( $n < 9$ ) clusters? A series of photoionization mass spectroscopic experiments of  $\text{Cs}_{(n+2m)}\text{O}_m$  showed that these oxygen-doped clusters have  $n$  delocalized electrons, which can apparently be described by the Jellium model as in pure alkali-metal clusters [11,12]. Thus it is natural to ask whether the electronic structures of  $\text{Al}_n\text{N}$  clusters can be described or explained by the Jellium model as in the alkali oxide clusters. Other interesting questions include: What is the critical cluster size range where the separate  $3s$  and  $3p$  “bands” overlap and the Jellium model starts to be valid for the  $\text{Al}_n\text{N}$  clusters? What is the implication of the geometrical evolution associated with the electronic structures?

Several experimental and theoretical studies have been focused on  $\text{Al}_n\text{N}_m$  clusters ( $n = 2-20, m = 1-3$ ) to

<sup>a</sup> e-mail: [ls.wang@pnl.gov](mailto:ls.wang@pnl.gov)

understand their electronic and structural properties [13–16]. Previously we reported a photoelectron spectroscopic study of the mononitrogen doped aluminum cluster anion  $\text{Al}_n\text{N}^-$  ( $n = 3$  and 4) and confirmed the electronic and geometrical structures and their high stability predicted by calculations [13–15]. A recent study was devoted to small  $\text{Al}_n\text{N}$  clusters for  $n$  up to 8 [16]. An interesting DFT study on  $\text{Al}_n\text{N}$  clusters suggested that the ionization potential decreases monotonically as the metallic component of the  $\text{Al}_n\text{N}$  cluster is increased. The electronic structure of  $\text{Al}_{12}\text{N}$ , in icosahedral structure ( $I_h$ ) with a central N atom, was found to be metallic [14]. It was proposed that the icosahedral  $\text{Al}_{12}\text{N}$  cluster has 41 valence electrons of which 5 electrons are contributed by the central nitrogen atom, one more than 40 required to reach a shell closing in the Jellium model. The chemistry of  $\text{Al}_{12}\text{N}$  should, therefore, be like that of an alkali atom. To prove this, a calculated low ionization potential for the icosahedral  $\text{Al}_{12}\text{N}$  was compared to alkali atoms and thus  $(\text{Al}_{12}\text{N})\text{Cl}$  was considered as an ionic molecule [14]. Recently a mass spectroscopy and theoretical investigation on reactivity of stable aluminum–nitrogen cluster species toward oxygen has been conducted, with particular emphasis placed on the applicability of both the Jellium model and a composite Jellium system on  $\text{Al}_2\text{N}^-$ ,  $\text{Al}_3\text{N}_2^-$ ,  $\text{Al}_5\text{N}_2^-$ ,  $\text{Al}_6\text{N}_3^-$ ,  $\text{Al}_8\text{N}_3^-$  and  $\text{Al}_9\text{N}_2^-$  [16].

In this contribution, we present a study on the electronic structure of a series of mononitrogen doped aluminum clusters  $\text{Al}_n\text{N}$  ( $n = 2–43$ ) using anion photoelectron spectroscopy (PES) [17]. This is a continuation of our research interest on  $\text{Al}_n\text{N}$  clusters [15]. Despite the previous works on small  $\text{Al}_n\text{N}$  clusters, little experimental spectroscopic information is available except for the  $\text{Al}_3\text{N}^-$  and  $\text{Al}_4\text{N}^-$  clusters [13–16]. PES is a valuable technique to probe the electronic structure and chemical bonding of gas-phase clusters [4,17]. In the current work, we report well-resolved PES data of  $\text{Al}_n\text{N}^-$  ( $n = 2–22$ ). We observed that  $\text{Al}_4\text{N}$  anion is a magic number in the mass spectrum and the magic cluster  $\text{Al}_{13}^-$  anion also appeared as a particularly strong peak in the  $\text{Al}_n^-/\text{Al}_n\text{N}^-$  anion mass spectra. An even-odd alternation of electron affinities was observed from the PES spectra for  $\text{Al}_n\text{N}$  clusters, suggesting a behavior of electron shell closing and opening. The evolution of the PES spectral patterns and the measured electron affinities could be interpreted by the Jellium model and compared with previous available theoretical calculations. The similarities between the PES spectrum of  $\text{Al}_n\text{N}^-$  and  $\text{Al}_{(n-1)}^-$  allow us to deduce and predict the electronic and relatively geometrical structures of  $\text{Al}_n\text{N}$  clusters based on the known electronic and geometrical structures of the corresponding  $\text{Al}_{(n-1)}$  clusters. We will address the questions mentioned above by comparison of photoelectron spectra of size selected  $\text{Al}_n\text{N}$  anions and pure aluminum anion clusters.

## 2 Experiment

The experiment was performed with a magnetic-bottle time-of-flight PES apparatus equipped with a laser va-

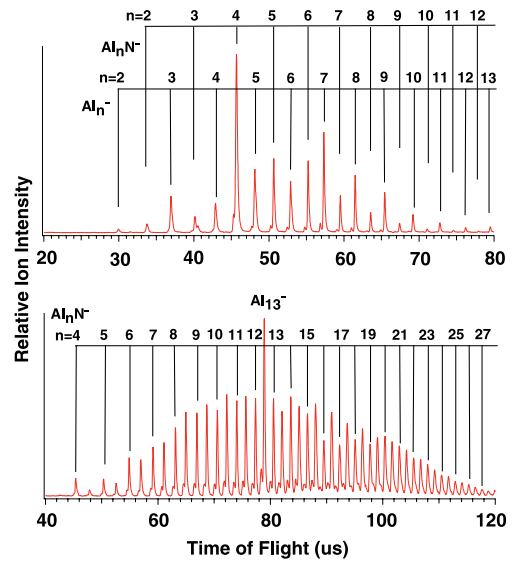


**Fig. 1.** Mass spectra of aluminum and aluminum nitride anion clusters, produced by laser vaporization of a pure Al target with a helium carrier gas containing 5%  $\text{N}_2$ .

porization cluster source. Details of the experiment have been described previously [17]. Briefly, the second harmonic output of a Q-switched Nd:YAG laser, typically at 10 mJ/pulse and 10 Hz repetition rate, was focused down to a 1 mm spot onto an Al or AlN disk target controlled by two stepping motors. A helium carrier gas pulse (10 atmosphere backing pressure) seeded with 5%  $\text{N}_2$  was delivered to the laser vaporization nozzle by a dual Jordan valve assembly. Clusters from the source underwent a supersonic expansion and collimated by a skimmer. Negatively charged clusters were extracted from the cluster beam perpendicularly and were analyzed by a time-of-flight mass spectrometer. The cluster anions of interest were mass-selected before photodetachment with one of the three photon energies: 355 nm (3.496 eV), 266 nm (4.661 eV), and 193 nm (6.424 eV). Photoelectron spectra were measured using a magnetic-bottle time-of-flight photoelectron analyzer with an electron kinetic energy resolution of  $\Delta E_k/E_k \sim 2.5\%$ . The spectrometer was calibrated with the known spectrum of  $\text{Cu}^-$  and  $\text{Rh}^-$ .

## 3 Experimental results

Figure 1 shows two mass spectra of the  $\text{Al}_n^-$  and  $\text{Al}_n\text{N}^-$  species, covering two different mass ranges. Regardless of the targets used (pure Al or AlN) or percentages of  $\text{N}_2$  in the helium carrier gas, we could only produce nitride clusters containing only one N dopant atom under our experimental conditions, owing to the strong N-N bond of the  $\text{N}_2$  molecule. In the small cluster range,  $\text{Al}_4\text{N}^-$  was found to be a magic number. In the higher mass range,  $\text{Al}_{13}^-$  stands out as the strongest mass peak.

Figure 2 shows the PES spectra of the  $\text{Al}_n\text{N}^-$  clusters with  $n = 2–22$  at 193 nm (6.424 eV). Overall the PES spectra of the small  $\text{Al}_n\text{N}^-$  clusters with  $n$  less than 8

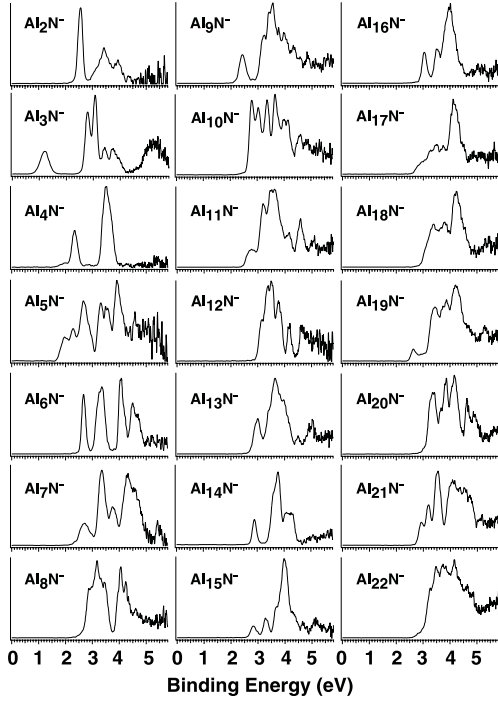
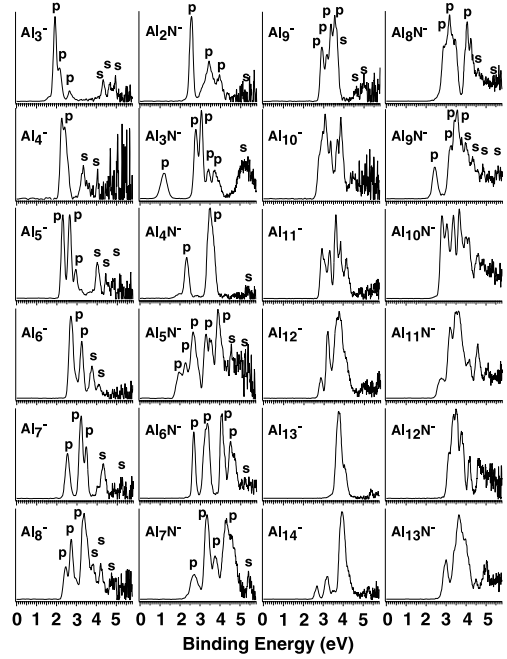


**Fig. 2.** Photoelectron spectra of  $\text{Al}_n\text{N}^-$  for  $n = 2-22$  at 193 nm (6.424 eV).

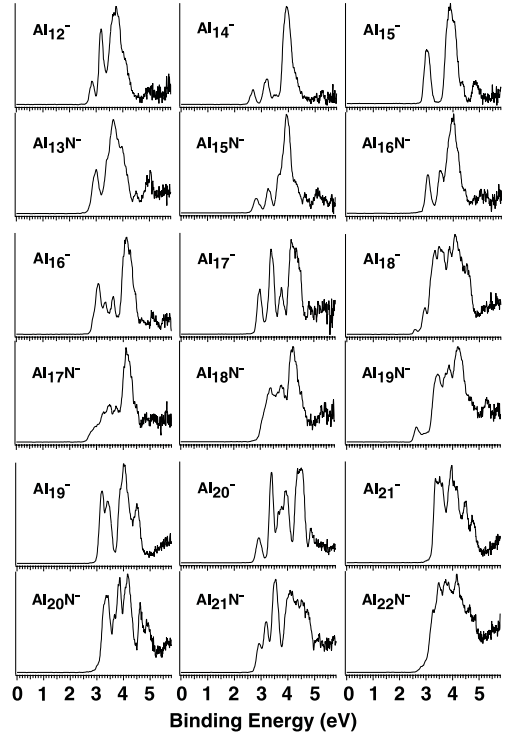
display well resolved features, whereas the PES spectra of larger  $\text{Al}_n\text{N}^-$  clusters with  $n > 8$  show more complicated features. For  $\text{Al}_n\text{N}^-$  with  $n = 22-43$ , the PES spectra look more congested and broadened with less distinct features and are not presented here.

Figure 3 compares the PES spectra of  $\text{Al}_n\text{N}^-$  with those of pure  $\text{Al}_{(n+1)}^-$  cluster at 193 nm for  $n = 2-13$ . With  $n$  below 10, the PES spectra of  $\text{Al}_n\text{N}^-$  have no indication to be similar to that of  $\text{Al}_{(n+1)}^-$  or  $\text{Al}_n^-$ , underlying their molecular nature. Starting from  $n = 10$  to 12, the PES spectra of  $\text{Al}_n\text{N}^-$  show some similarity to those of  $\text{Al}_{(n+1)}^-$ . The congested spectral features in  $\text{Al}_{10}\text{N}^-$  evolved into a relatively narrow band with strong intensity in  $\text{Al}_{12}\text{N}^-$ , analogous to the spectral evolution from  $\text{Al}_{11}^-$  to  $\text{Al}_{13}^-$ , which exhibits a very narrow spectral band. There was no clear similarity between the PES spectra of  $\text{Al}_{13}\text{N}^-$  and  $\text{Al}_{14}^-$ , but surprisingly resemblance seems to exist in the PES spectra of  $\text{Al}_{13}\text{N}^-$  and  $\text{Al}_{12}^-$ .

In Figure 4, we compare the 193 nm PES spectra of  $\text{Al}_{(n-1)}^-$  and  $\text{Al}_n\text{N}^-$  for  $n = 13, 15-22$ . Note the apparent similarity between the spectra of  $\text{Al}_n\text{N}^-$  and those of  $\text{Al}_{(n-1)}^-$ . There is a common intense feature in the PES spectra of  $\text{Al}_n\text{N}^-$  for  $n = 13$  to at least  $n = 18$ . This intense feature is characteristic of the PES spectrum of the icosahedral  $\text{Al}_{13}^-$ , but it is also clearly shown in the spectra of  $\text{Al}_{12}^-$ ,  $\text{Al}_{14}^-$  and  $\text{Al}_{15}^-$ , which were all shown to have geometrical structures derived from the  $I_h$   $\text{Al}_{13}^-$  [18]. Especially, the PES spectrum of  $\text{Al}_{15}\text{N}^-$  looks almost identical to that of  $\text{Al}_{14}\text{N}^-$  both in the general PES spectral pattern and binding energies.



**Fig. 3.** Comparison of the photoelectron spectra of  $\text{Al}_{(n+1)}^-$  (first and third columns) and  $\text{Al}_n\text{N}^-$  (second and fourth columns) for  $n = 2-13$  at 193 nm (6.424 eV).



**Fig. 4.** Comparison between the 193 nm spectra of  $\text{Al}_{(n-1)}^-$  and  $\text{Al}_n\text{N}^-$  for  $n = 13, 15-22$ .

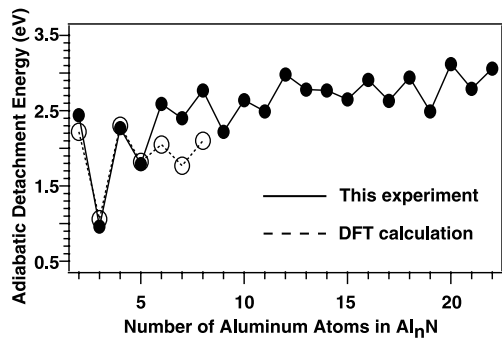


**Fig. 5.** Measured adiabatic detachment energies for  $\text{Al}_n\text{N}^-$  ( $n = 2-22$ ) (solid line with dot) versus the number of Al atoms. DFT results for  $n = 2-8$  (open circle) are taken from reference [16].

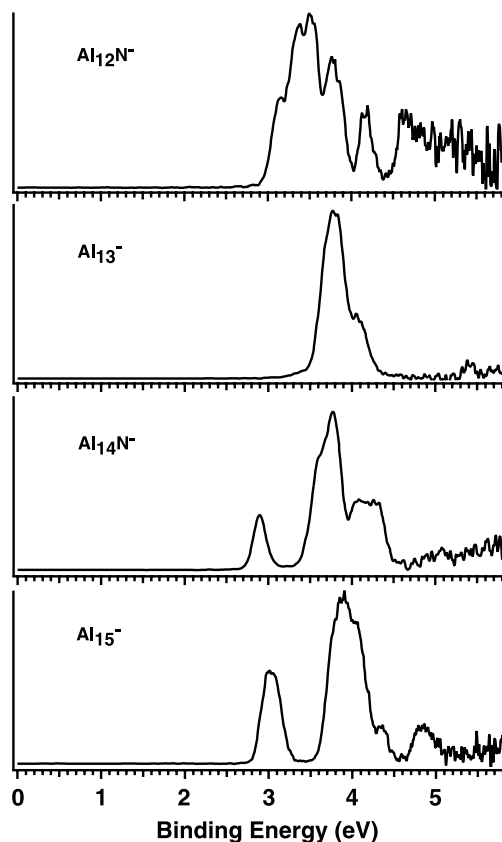


**Fig. 6.** Comparison between the photoelectron spectra of  $\text{Al}_{(n+1)}^-$  and that of  $\text{Al}_n\text{N}^-$  for  $n = 12$  and  $14$  at  $193$  nm.

The adiabatic detachment energies (ADE) for  $\text{Al}_n\text{N}^-$  with  $n = 2-22$  were measured from the onset of the lowest binding energy feature of the PES spectra. These values, which correspond to the electron affinities (EA) of the neutral clusters, are shown in Figure 5, where they are compared with the available DFT results [16].

Figure 6 shows a comparison of the  $193$  nm PES spectra between  $\text{Al}_{(n+1)}^-$  and  $\text{Al}_n\text{N}^-$  for  $n = 12$  and  $14$ . Here the PES spectra of  $\text{Al}_n\text{N}^-$  were identified to be similar to that of  $\text{Al}_{(n+1)}^-$  in general pattern and trend (also see

Fig. 3). The similarity between the spectra of  $\text{Al}_{14}\text{N}^-$  and  $\text{Al}_{15}^-$  are more obvious, although the threshold peak in the spectrum of  $\text{Al}_{14}\text{N}^-$  seems to be weaker and sharper than that in the  $\text{Al}_{15}^-$  spectrum.

## 4 Discussion

The PES spectra shown in Figures 2, 3, 4 and 6 represent detachment transitions from the anions to the various states of the neutrals. They reveal information about the electronic structure and chemical bonding of these clusters. However, except for  $\text{Al}_n\text{N}$  clusters with  $n$  up to 8 [13–16] and pure  $\text{Al}_n$  clusters [18–20], there have been few theoretical studies on the structure and bonding of these species. In particular, the electronic structures of these species are extremely complex and very little is known for this series of species except for  $\text{Al}_3\text{N}$  and  $\text{Al}_4\text{N}$  and their anions [13–16]. Therefore, here we will discuss only qualitatively the trend of the spectra and the possible structural implications on the basis of the electronic shell model and the available calculations.

### 4.1 Even-odd alternation of electron affinities in small $\text{Al}_n\text{N}$ clusters

In general, the detailed spectral features of the  $\text{Al}_n\text{N}^-$  clusters are different from those of pure  $\text{Al}_n^-$  clusters in the small size regime (Fig. 3), indicating that the chemical bonding and geometrical structures in the small N doped Al clusters are different from that in  $\text{Al}_n$  clusters. A strong even-odd alternation of electron affinities in the PES spectra of  $\text{Al}_n\text{N}^-$  clusters was observed (Fig. 5), suggesting that there exist electronic shell opening and closing alternation in these clusters.  $\text{Al}_n\text{N}$  clusters with odd  $n$  have lower EAs, indicating they are closed shell systems. The PES spectra of anions of these clusters exhibit a clear energy gap (HOMO-LUMO gap), which appears to be the largest in  $\text{Al}_3\text{N}^-$ . The high EAs of the even  $n$  clusters indicate that their anions are closed shell, i.e., the neutrals are open shell with one unpaired electron. The observed stability of  $\text{Al}_2\text{N}^-$  to oxygen [16] and the magic number behavior of  $\text{Al}_4\text{N}^-$  in the mass spectrum are consistent with this observation. Like in the PES spectra of  $\text{Al}_n$  cluster anions [4], the features from  $p$ - and  $s$ -derived molecular orbitals (MOs) in the PES spectra of  $\text{Al}_n\text{N}^-$  are labeled in Figure 3 with “ $p$ ” and “ $s$ ”, respectively. The  $s$  features are characterized by their high binding energies and low detachment cross sections. It could qualitatively be seen that the  $p$ - and  $s$ -derived features in the PES spectrum of  $\text{Al}_8\text{N}^-$  already start to overlap partially and eventually form a unified and relatively narrow  $s-p$  hybridized band in  $\text{Al}_{12}\text{N}^-$ . Thus the  $s-p$  hybridization behavior as a function of size in the mono-N doped  $\text{Al}_n\text{N}$  clusters is similar to that as in the  $\text{Al}_n$  clusters [4]. Hence in small  $\text{Al}_n\text{N}$  clusters, Al may be considered as monovalent due to the large energy gap between  $3s$  and  $3p$  orbitals of the Al-atom ( $3.6$  eV [5]).

## 4.2 Evidence of Jellium-like $\text{Al}_n\text{N}^-$ clusters

In our study of Al clusters [4], we observed an abrupt change in the PES spectra from a complicated multi-feature spectrum for  $\text{Al}_{12}^-$  to a relatively simple band for  $\text{Al}_{13}^-$  (Fig. 3), which was confirmed to be an ideal icosahedron through a combined experimental and theoretical study [18, 19]. The PES spectra of  $\text{Al}_{14}^-$ ,  $\text{Al}_{15}^-$ ,  $\text{Al}_{16}^-$ ,  $\text{Al}_{17}^-$ ,  $\text{Al}_{18}^-$ , and  $\text{Al}_{19}^-$  all maintained the main feature of  $\text{Al}_{13}^-$  besides a few weaker low energy features (see Figs. 4 and 6). These clusters were shown to be either capped icosahedra or a bi-icosahedron in  $\text{Al}_{19}^-$  [18, 19], which also exhibits a major electronic shell closing. In the large  $\text{Al}_n\text{N}^-$  clusters with  $n$  over 11, we observed similar PES spectra between  $\text{Al}_n\text{N}^-$  and  $\text{Al}_{(n-1)}^-$  (Fig. 4), suggesting that the N-doped clusters can also be described by the electron shell model and may possess similar atomic structures as the pure aluminum clusters. Our data suggest that N in the  $\text{Al}_n\text{N}$  cluster acts as a three-electron acceptor to form  $\text{N}^{3-}$  formally. Thus the  $\text{Al}_n\text{N}^-$  clusters can be best described as  $(\text{AlN})\text{Al}_{(n-1)}^-$ , i.e., a diatomic AlN molecule weakly interacting with a pure metallic Al cluster. This observation is important in considering the atomic structures of the N-doped Al clusters. The presence of the AlN unit seems to have very little perturbation to the electronic structure of the remaining Jellium-like  $\text{Al}_{(n-1)}^-$  clusters. Theoretically no detailed electronic and geometrical structure information is available for  $\text{Al}_n\text{N}^-$  except for  $\text{Al}_3\text{N}^-$  and  $\text{Al}_4\text{N}^-$  [15]. Nevertheless, from their well-resolved PES spectra and comparison with that of Al cluster anions, more symmetric structures with icosahedral-like cores for  $\text{Al}_n\text{N}$  in the size range of  $n = 12, 14-20$  are likely. Similar to  $\text{Al}_{13}^-$ ,  $\text{Al}_{12}\text{N}^-$  may also possess a highly symmetric  $I_h$  or distorted  $I_h$  structure.

## 4.3 EA vs. cluster size

The well-defined and sharp onset of the threshold PES feature allowed us to obtain fairly accurate ADEs or EAs for the corresponding neutral  $\text{Al}_n\text{N}$  species, as plotted in Figure 5. The EAs exhibit strong size variation in the smaller size regime from  $\text{Al}_2\text{N}$  to about  $\text{Al}_{12}\text{N}$ . Some of the EA variations in the large size regime correlate to both electronic and geometric structural effects. For example, the EA of  $\text{Al}_{12}\text{N}$  and  $\text{Al}_{20}\text{N}$  exhibits local maximums (Fig. 5), which may correlate to their highly symmetric structure mentioned above, in addition to the fact that their anions are closed shell. The EAs for  $\text{Al}_n\text{N}$  ( $n = 2-8$ ) have been calculated using DFT method [16] and are compared with the experimental data in Figure 5. The calculated EAs for the small clusters ( $n = 2-5$ ) are in excellent agreement with the experiment. The agreement for the larger clusters deteriorates, but the general trend is in good accord with the experimental data.

Interestingly the even-odd alternations of the EA can be seen clearly in two size ranges, one between  $n = 2$  to 12 and another between  $n = 15$  to 22. The EA decreases with  $n$  from  $n = 12-15$ , suggesting the opening of a new

electronic sub-shell. The maximum at  $n = 20$ , i.e.  $\text{Al}_{20}\text{N}^-$  or  $(\text{AlN})\text{Al}_{19}^-$ , is because  $\text{Al}_{19}^-$  with 58 free electrons is a major shell closing [4].

## 4.4 From $\text{Al}_{12}\text{N}^-$ to $\text{Al}_{20}\text{N}^-$ : spectroscopic trend and implication for structural evolution

As shown in Figure 4, the resemblance between the spectra of  $\text{Al}_n^-$  and  $\text{Al}_{(n+1)}\text{N}^-$  clusters starts from  $\text{Al}_{13}\text{N}^-$ . The spectrum of  $\text{Al}_{12}\text{N}^-$  does not exhibit much similarity to  $\text{Al}_{11}^-$ . Rather, it is more comparable to  $\text{Al}_{13}^-$  (Fig. 6), even though the spectrum of  $\text{Al}_{12}\text{N}^-$  has more resolved features than that of  $\text{Al}_{13}^-$ . The high binding energy and high density of states in the  $\text{Al}_{12}\text{N}^-$  spectrum are both similar to that of  $\text{Al}_{13}^-$ , which may indicate  $\text{Al}_{12}\text{N}^-$  possesses a similar symmetry as the icosahedral  $\text{Al}_{13}^-$ . Now an interesting question arises from this structural implication. Where should the N dopant atom locate in the icosahedron-like  $\text{Al}_{12}\text{N}^-$ , in the center or on the outer shell? Several factors determine if the N atom would be feasible to be inside to form an  $I_h \text{N}@\text{Al}_{12}$ . The first is the electronegativity of N, which determines if N is likely to lose its valence electrons to participate in metallic bonding. Secondly, the preferred coordination number of the N atom. N has high electronegativity, and thus is a poor electron donor. It also does not prefer high coordination. Both of these factors indicate that N is unlikely to be in the center of an  $I_h \text{Al}_{12}$  to form an  $I_h \text{N}@\text{Al}_{12}$ , like that of  $\text{Al}_{13}^-$ . In fact, in small  $\text{Al}_n\text{N}$  cluster for  $n$  up to 6, N indeed prefers to accept additional electrons from the peripheral Al atoms like those in bulk AlN, where N can be formally viewed as  $\text{N}^{3-}$ . Although the DFT calculations suggested that the N atom is surrounded by Al atom in the  $\text{Al}_n\text{N}$  clusters at its ground state for  $n$  up to 8, the coordination number does not exceed 7 even in  $\text{Al}_8\text{N}$  [16]. The atomic size of the impurity atom is also a key factor to determine if it can be stable in the center of the icosahedral structure. Earlier studies on the ground state of  $\text{Al}_{13}$  found it to be icosahedral with a radial bond length of about 2.7 Å [14, 20–22]. The studies on  $\text{Al}_{12}\text{B}^-$  or  $\text{Al}_{12}\text{C}$  have shown that when an Al atom in  $\text{Al}_{13}$  is replaced by a B or C atom, the smaller atom prefers to occupy the central site despite its high electronegativity [22]. In the present case, the N atom has a higher electronegativity and its atomic radius is even smaller than that of B and C atoms. Therefore it is expected that the geometry of an icosahedral  $\text{Al}_{12}\text{N}$  cluster with the N atom occupying the central site may not be as stable comparing to  $\text{Al}_{12}\text{B}^-$ ,  $\text{Al}_{12}\text{C}$ , and  $\text{Al}_{13}^-$  [21], even though a previous DFT calculation has considered an  $I_h \text{Al}_{12}\text{N}$  cluster [14]. As shown below, the stronger AlN bond relative to  $\text{Al}_2$  [14, 16, 23] really favors a segregated  $(\text{AlN})\text{Al}_{(n-1)}^-$  type structure for the large clusters, again suggesting that  $\text{Al}_{12}\text{N}^-$  is unlikely to have a  $\text{N}@\text{Al}_{12}$  structure. It is worthwhile to mention that recent DFT calculations on  $\text{Al}_{12}\text{C}^-$  and its neutral found that in the ground state, the icosahedron with C sitting at the center of  $\text{Al}_{12}\text{C}$  is the lowest energy structure, but this is not the case for the anion, that is, with one

extra electron adding into  $\text{Al}_{12}\text{C}$ , C will prefer to stay on the surface of a heavily distorted structure [24,25].  $\text{Al}_{12}\text{N}$  is isoelectronic with  $\text{Al}_{12}\text{C}^-$ , again indicating that  $\text{Al}_{12}\text{N}$  is unlikely to have a  $\text{N}@Al_{12}$  type structure, i.e. N is likely bonded to the surface of the cluster in a distorted icosahedral structure.

We speculate that for  $n > 12$  except for  $n = 14$  the  $\text{Al}_n\text{N}$ -clusters can be viewed as  $(\text{AlN})\text{Al}_{(n-1)}^-$ , where the strongly bonded AlN diatomic unit seems to have very little perturbation to the electronic structure of  $\text{Al}_{(n-1)}^-$  (Fig. 4). These clusters may possess icosahedral-like structures with an AlN unit on its surface.

If we use the same argument mentioned above,  $\text{Al}_{14}\text{N}^-$  should be formulated as  $I_h\text{-Al}_{13}^- + \text{AlN}$ . However, there was an extra feature in the PES spectrum of  $\text{Al}_{14}\text{N}^-$  besides the main features, which do show resemblance to that of  $\text{Al}_{13}^-$  (Fig. 6).  $\text{Al}_{13}^-$  has the highest symmetry and highest electronic degeneracy. The extra feature in  $\text{Al}_{14}\text{N}^-$  may be caused by the breaking of the  $I_h$  symmetry of  $\text{Al}_{13}^-$  due to the presence of the AlN unit. The fact that the spectrum of  $\text{Al}_{14}\text{N}^-$  is similar to that of  $\text{Al}_{15}^-$  may suggest that the structural distortion in  $\text{Al}_{14}\text{N}^-$  is similar to that of  $\text{Al}_{15}^-$ , which has a bi-capped icosahedral structure [18]. Thus, we could conclude that starting from  $\text{Al}_{13}\text{N}$  to at least  $\text{Al}_{20}\text{N}$  the N dopant atom does not stay inside the Al clusters. They can be viewed electronically as an AlN unit interacting with an  $\text{Al}_{(n-1)}^-$  cluster. Structurally they might be viewed as N bound to the surface of the Al clusters with low coordination.

## 5 Conclusion

In conclusion, we have reported a photoelectron spectroscopic investigation of a series of mononitrogen doped aluminum clusters  $\text{Al}_n\text{N}^-$  ( $n = 2-22$ ). Well-resolved PES spectra revealed structural and electronic evolution and chemical bonding in  $\text{Al}_n\text{N}^-$  and  $\text{Al}_n\text{N}$ . The PES spectra and the electronic structure of the N-doped clusters are compared to pure Al clusters. For  $n \leq 9$ , the aluminum atoms in the N-doped clusters behave as monovalent atoms, similar to that of small Al clusters [4]. The critical cluster size range where the separate  $s$  and  $p$  “bands” overlap and hybridize is from  $\text{Al}_9\text{N}$  to  $\text{Al}_{11}\text{N}$ , and the Jellium model starts to be operative for the large  $\text{Al}_n\text{N}$  clusters. The most interesting observation for these clusters is the spectral similarity between an  $\text{Al}_{(n-1)}^-$  cluster and an  $\text{Al}_n\text{N}^-$  cluster. These clusters can be viewed as  $(\text{AlN})\text{Al}_{(n-1)}^-$ . This observation also suggests that the N dopant atom is unlikely to be in the center of the Al clusters in these species. Thus the large  $\text{Al}_n\text{N}^-$  clusters can be described by the electron shell model similarly as the Al clusters, weakly perturbed by an AlN unit. This ob-

servations is consistent with the observation of compound clusters in cesium oxide system previously [11,12]. The detailed electronic structure information and the implications for geometrical structures would be ideal to compare to further theoretical investigations.

This research was supported by the National Science Foundation (DMR-0095828) and performed at the W.R. Wiley Environmental Molecular Sciences Laboratory, a national scientific user facility sponsored by the DOE’s Office of Biological and Environmental Research and located at Pacific Northwest National Laboratory, operated for the DOE by Battelle. This article is dedicated to the memory of Prof. Bijan K. Rao.

## References

1. W.A. de Heer, Rev. Mod. Phys. **65**, 611 (1993)
2. M. Brack, Rev. Mod. Phys. **65**, 677 (1993)
3. N.W. Ashcroft, N.D. Mermin, *Solid State Physics* (Holt, Rinehart, and Winston, New York, 1976)
4. X. Li, H. Wu, X.B. Wang, L.S. Wang, Phys. Rev. Lett. **81**, 1909 (1998)
5. C.E. Moore, in *Atomic Energy Levels*, Natl. Bur. Stand. (U.S.) Circ. (U.S. GPO, Washington, D.C., 1971), Vol. I
6. W.D. Knight et al., Phys. Rev. Lett. **52**, 2141 (1984)
7. W. Ekardt, Phys. Rev. B **29**, 1558 (1984)
8. M.L. Cohen et al., J. Phys. Chem. **91**, 3141 (1987)
9. M. Ueno, A. Onodera, O. Shimomura, K. Takemura, Phys. Rev. B **45**, 10123 (1992)
10. F.A. Ponce, D.P. Bour, Nature **386**, 351 (1997)
11. T. Bergmann, H. Limberger, T.P. Martin, Phys. Rev. Lett. **60**, 1767 (1988)
12. T. Bergmann, T.P. Martin, J. Chem. Phys. **90**, 2848 (1989)
13. P.V.R. Schleyer, A.I. Boldyrev, J. Chem. Soc. Chem. Commun. 1536 (1991)
14. S.K. Nayak, S.N. Khanna, P. Jena, Phys. Rev. B **57**, 3787 (1998)
15. S.K. Nayak, B.K. Rao, P. Jena, X. Li, L.S. Wang, Chem. Phys. Lett. **301**, 379 (1999)
16. B.D. Leskiw, A.W. Castleman Jr, C. Ashman, S.N. Khanna, J. Chem. Phys. **114**, 1165 (2001)
17. L.S. Wang, H.S. Cheng, J. Fan, J. Chem. Phys. **102**, 9480 (1995)
18. J. Akola, M. Manninen, H. Hakkinen, U. Landman, X. Li, L.S. Wang, Phys. Rev. B **60**, R11297 (1999)
19. J. Akola, M. Manninen, H. Hakkinen, U. Landman, X. Li, L.S. Wang, Phys. Rev. B **62**, 13216 (2000)
20. B.K. Rao, P. Jena, J. Chem. Phys. **111**, 1890 (1999)
21. S.N. Khanna, P. Jena, Phys. Rev. Lett. **69**, 1664 (1992)
22. X.G. Gong, V. Kumar, Phys. Rev. Lett. **70**, 2078 (1993)
23. K.P. Huber, G. Herzberg, *Constants of Diatomic Molecules* (Nostrand-Reinhold, New York, 1979)
24. B.K. Rao, P. Jena, J. Chem. Phys. **115**, 778 (2001)
25. S.F. Li, X.G. Gong, Phys. Rev. B **70**, 075404 (2004)